1064-nm Sensitive Organic Photorefractive Composites

Koeber, Sebastian; Prauzner, Jacek; Salvador, Michael; Kooistra, Floris B.; Hummelen, Jan C.; Meerholz, Klaus

Published in:
Advanced materials

DOI:
10.1002/adma.200903005

Publication date:
2010

1064-nm Sensitive Organic Photorefractive Composites

By *Sebastian Köber, Jacek Prauzner, Michael Salvador, Floris B. Kooistra, Jan C. Hummelen,* and *Klaus Meerholz**

Noninvasive, depth-resolved mapping of 3D biological structures by nonionizing optical radiation is one of the most challenging and promising methods of biomedical imaging.[1,2] The properties of the biological structure hereby determine the wavelength of the optical radiation utilized for the imaging process. While the favorable scattering properties of dermal tissue in the near infrared (NIR) demand light-sources operating at the ''skin transparency window'' of 700–900 nm, wavelenghts near 1 μm are particularly suited for ophthalmic imaging applications, due to its high penetration depth into the choroid of the human eye.[3] Practicable methods to acquire 3D images are confocal microscopy (CM), optical coherence tomography (OCT) and dynamic holography. The latter technique (excluding digital holography[4]) offers the advantage of a purely optical whole-field reconstruction of 2-dimensional image slices, in comparison to point-like scanning in three dimensions and subsequent computations of OCT and CM. Image formation through the holographic optical coherence imaging (HOCI)-technique relies on coherence-gated discrimination of information bearing ballistic photons from multiple scattered photons emerging from the illuminated specimen under investigation, through interference with a reference-beam in a reversible holographic medium. The photorefractive effect is thereby considered to be the most promising method, providing reconfigurable real-time updateable holographic memory. Due to the small fraction of ballistic photons backscattered from the specimen, HOCI imposes stringent requirements regarding light intensity and recording speed on the holographic material to be operated under in vivo imaging conditions. In the current literature, no photorefractive material sensitive at wavelengths around 1 μm, e.g., compound semiconductor materials such as GaAs, InP or CdTe[5] or crystalline photorefractive materials such as Cu- or Fe-doped $LiNbO_3$,[6] or Te-doped $Sn_2P_2S_6$,[7] combines large nonlinearities with sufficiently fast response-times under low intensity illumination to be useful for imaging purposes. Typical drawbacks of crystalline materials are moreover their relatively high price due to their difficult growth conditions.

Polymeric photorefractive composite (PPC) materials offer the advantages of low cost, ease and flexibility of fabrication, and—in case of low glass-transition temperature materials ($T_g < RT$)—large nonlinearities due to the orientational enhancement effect.[8] Low-T_g PPCs with fast holographic response were successfully demonstrated in the visible and near-infrared range (633–975 nm),[9,10] recent materials were shown to be sufficiently sensitive for depth-resolved imaging of biological samples.[11] In contrast, at longer wavelengths, PPCs sensitized with carbon nanotubes, a ruthenium(II) complex, or cyanine dye J-aggregates (1064 nm[12]) or HgS and PbS nanocrystals (1310 nm,[13] 1550 nm[14]), usually have slow response times in the order of tens of seconds and limited diffractive properties. Sensitization through two-photon absorption dyes (1550 nm[15]) requires the use of high power, pulsed laser sources. In this work, we demonstrate for the first time subsecond response times and complete internal diffraction efficiency at 1064 nm. The performance of the materials corresponds to a factor 44 enhanced response time and an increase of the sensitivity by a factor of 34 compared to similar materials sensitive in this particular spectral range.

The photorefractive effect in dc-field biased, low-T_g organic materials involves charge-carrier photogeneration in the bright regions of an interference pattern and the subsequent displacement of the mobile charge due to field induced drift. The separation of charge centers leads to the formation of an internal space-charge field E_{SC}, which is phase-shifted relative to the interference pattern. In low-T_g materials, electro-optic chromophores are reoriented along the total field E_T, which is the vectorial sum of E_{SC} and the applied field E_{ext}.[8] The change of refractive index Δn is then given through the quadratic electro-optic (Kerr−) effect and modulated uniaxial birefringence. A stepwise description of the photorefractive effect in organic composite materials and its underlying photo-physical details can be found in recent bookchapters[16,17] and review/feature articles.[9,18] The phase-shift ϕ between the refractive index modulation and the interference pattern gives rise to an energy exchange between the write beams, leading to amplification of one beam at the cost of the other while propagating through the photorefractive medium. A quantitative measure for this two-beam coupling (2BC) effect is the gain coefficient Γ (see Experimental Section), which depends on the refractive index amplitude and the phase shift through $\Gamma \approx \Delta n \sin \phi$.

The PPCs described in this work are based on the polymeric hole-conducting charge-transporting agent (CTA) Poly-(*N*,*N*′-bis(4-hexylphenyl)-*N*′-(4-(9-phenyl-9*H*-fluoren-9-yl)-phenyl)-4,4'-benzidine) (PF6-TPD, ca. 50 wt %; Fig. 1a),[19] the electro-optic activity is provided by an eutectic mixture of chromophores, 2,5-dimethyl-(4-*p*-nitrophenylazo)-anisole (DMNPAA; Fig. 1b) and 3-methoxy-(4-*p*-nitrophenylazo)-anisole (MNPAA; Fig. 1c) (25/25 wt %). An important feature is that the ionization potential of the chromophores is higher than that of the CTA, thus, the chromophores do not constitute hole traps, which would cause the temporal response of the materials to deteriorate.

The key ingredient that determines the spectral response of the PPC is the sensitizer. In this work, we use the fullerene derivative [84]PCBM (Fig. 2)[20] and the Ni-dithiolene complex TT-2324

[*] Prof. K. Meerholz, S. Köber, J. Prauzner, Dr. M. Salvador
Chemistry Department, University of Cologne
Luxemburger Str.116, 50939 Cologne (Germany)
E-mail: klaus.meerholz@uni-koeln.de
Dr. F. B. Kooistra, Prof. J. C. Hummelen
Stratingh Institute for Chemistry and Zernike Institute for Advanced Materials
University of Groningen
Nijenborgh 4, 9747 AG Groningen (The Netherlands)

DOI: 10.1002/adma.200903005

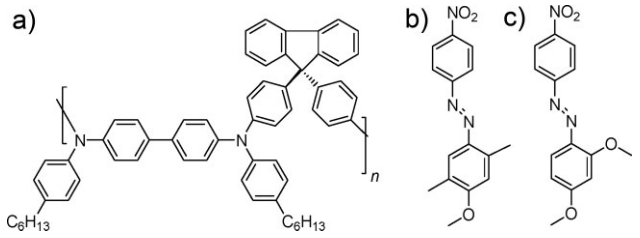

Figure 1. Chemical structures of the hole-conductor PF6-TPD a) and electro-optic chromophores DMNPAA b) and MNPAA c). The materials were synthesized in the chemistry labs of the University of Cologne. A detailed treatment of the synthesis aspects and structural characterization of the PF6-TPD-polymer is topic of a forthcoming publication [19].

(Fig. 3) as sensitizing agent. Both sensitizers are strong electron acceptors ([84]PCBM = −0.79 V, TT-2324 = −0.50 V vs. ferrocene/ferrocinium) as determined by cyclic voltammetry in acetonitrile. The sensitizers showed excellent compatibility with the polymer/chromophore mixture. The photorefractive devices were prepared by melt-pressing the polymeric material between two indium tin oxide (ITO)-coated glass sheets to a thickness of $d = 106\ \mu m$, ensured by glassy spacer beads. The glass transition temperature was $T_g = 6$–$7\ ^\circ C$ in all cases. The absorption coefficients of the bulk composites are listed in Table 1.

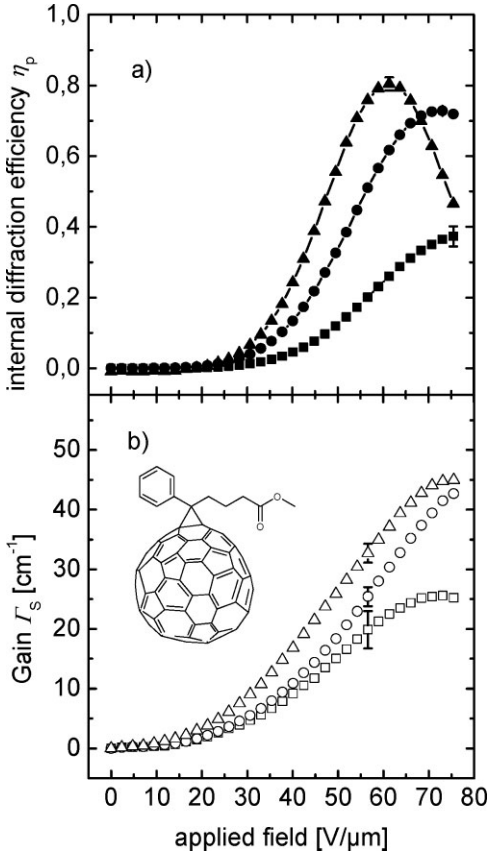

Figure 2. Steady-state internal diffraction efficiency η_P (a), solid symbols, and two-beam coupling gain Γ_S (b), open symbols, as function of the applied electric field for 1 wt % (■), 3 wt % (●), and 5 wt % (▲) [84]PCBM. Inset: chemical structure of [84]PCBM (only one isomer of the mixture drawn).

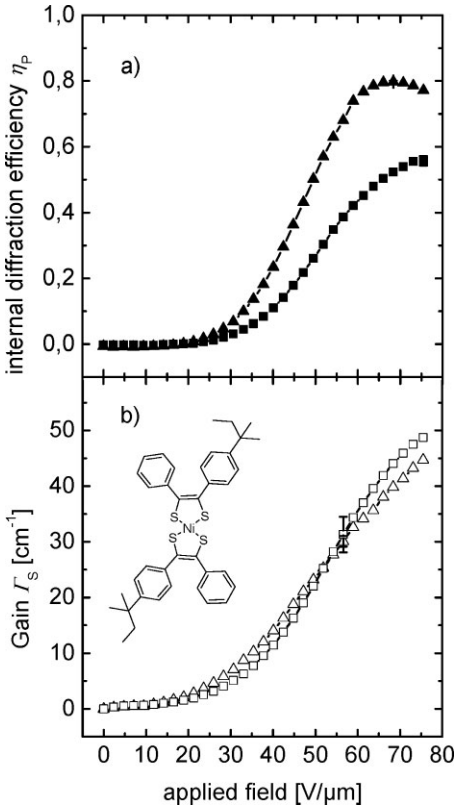

Figure 3. Field dependent internal diffraction efficiency η_P (a), solid symbols, and gain Γ_S (b), open symbols, for 1 wt % TT-2324 (■), and 5 wt % TT-2324 (▲). Inset: chemical structure of TT-2324.

The field-dependent internal diffraction efficiency η_P (see Experimental Section) for the two concentration series of [84]PCBM and TT-2324 are depicted in Figure 2 and 3, respectively. In both cases, the diffraction efficiency first increases with increasing field, overmodulates and finally decreases, in agreement with Kogelnik's formula,[21] the point of overmodulation corresponding at the employed geometry to a refractive index modulation of $\Delta n = 4.3 \times 10^{-3}$. For reference purposes, we will use the field $E_{ext} = 57\ V\,\mu m^{-1}$, which is below the field of overmodulation for even the most sensitive PPCs in this study.

The direct comparison of the PR performance of the materials sensitized by the two sensitizers yields higher internal diffraction efficiency values for the 1 wt % TT-2324 (38%) compared with 1 wt % [84]PCBM (20%). We attribute this to the higher molecular

Table 1. Physical properties of the measured PPCs: absorption coefficient α_{1064}, internal diffraction efficiency η_P, and gain coefficient Γ_s at steady-state conditions and τ_S-values from time-resolved measurements at $E_{ext} = 57\ V\,\mu m^{-1}$ and $1\ W\,cm^{-2}$ irradiance.

[84]PCBM [wt %]	α_{1064} [cm^{-1}]	η_P [%]	Γ_s [cm^{-1}]	τ_S [ms]
1	27 ± 1	20.1 ± 2.4	19.9 ± 3.1	174 ± 23
3	31 ± 2	51.0 ± 3.7	25.4 ± 1.6	54 ± 4
5	42 ± 2	75.9 ± 3.6	32.7 ± 1.6	36 ± 2
TT-2324 [wt %]				
1	42 ± 1	38.7 ± 0.9	31.3 ± 3.2	138 ± 11
5	120 ± 1	68.1 ± 1.8	30.1 ± 0.9	70 ± 5

mass of [84]PCBM ($M = 1199\,g\,mol^{-1}$) and, thus, a lower density of sensitizer molecules in the PPC as compared to the TT-2324 ($M = 683\,g\,mol^{-1}$). In addition, the absorption of the TT-2324 sensitizer at the recording wavelength is higher (42 vs. 27 cm^{-1}; see Table 1). For the 5 wt % sensitized materials, 76% and 68% internal diffraction efficiency was obtained for [84]PCBM and TT-2324, respectively. These results point to an asynchronous evolution of the performance of the materials with increased sensitizer doping, which is most likely due to the unfavorable strong increase of the absorption of the TT-2324 sensitized composite.

The 2BC-gain values were found to behave differently for the investigated sensitizers. As depicted in Figure 2b, Γ_s increased within the series from 1 wt % [84]PCBM to 5 wt % [84]PCBM, which, in concert with increasing Δn, indicates a similar phase-shift ϕ for all materials. The phase-shift for 3 wt % and 5 wt % [84]PCBM was calculated according to ref. [22] from Δn_p and Γ_s to be $18^\circ \pm 1^\circ$ and $17^\circ \pm 1^\circ$, respectively. By contrast, for the TT-2324 materials the gain was found to be independent of the sensitizer content. This finding indicates a decrease of the phase-shift when increasing the sensitizer content, which is equivalent to a reduced hole-displacement distance. These results indicate a strong influence of the TT-2324 density on the trapping landscape within the PPC.

For imaging applications under real-time conditions, the dynamic build-up of the refractive index grating under low illumination intensities is of paramount importance. In Figure 4 the response times τ_5 (see Experimental Section) of the [84]PCBM series are depicted as a function of the external write-beam intensity. The dynamic response of the materials scales sublinearly with intensity for all three sensitizer concentrations (slope ca. 0.95 ± 0.04 in all cases), which is indicative of a direct connection of the dynamic build-up with the photoconductivity of the sample alone.[23] Since the chromophore rotation is independent of illumination intensity, this clearly excludes rotational mobility limitations on the dynamic response for all investigated materials. Similar trends were observed with the TT-2324 sensitized materials. Response times τ_5 of all materials under 1 $W\,cm^{-2}$ irradiance and $E_{ext} = 57\,V\,\mu m^{-1}$ are listed in Table 1. The formation of gratings in the materials were fully reversible, the decay of the holograms after switching off both write-beams were monitored in each case. To estimate the response time for the erasure process (τ_{5e}), gratings written in the blend sensitized with 1 wt % TT-2324 were erased by uniform illumination from write-beam 1 after 160 s of grating formation time. The ratio of τ_{5e}/τ_5 was found to be 1.4 (after correcting for the intensity difference of factor 2 between grating writing and erasure). It should be pointed out, that grating erasure with an independent erasure beam of shorter wavelength (and hence higher absorption) would shift this ratio to more favorable ratios below unity. For write-erase cycles based on this procedure, the reader is referred to ref. [24].

The comparison of the composites presented in this work with 1064 nm sensitive materials based on organic high-T_g third-order nonlinear photorefractive materials reveals a dramatic reduction in response time. In case of a material sensitized with 0.43 wt % carbon nanotubes[25] τ_1 was estimated from a temporal plot of the read beam depletion upon grating build-up to be $\tau_1 = 1.2$ s for an irradiance of 0.3 $W\,cm^{-2}$ and an applied field of 79 $V\,\mu m^{-1}$. The response time doubles according to the authors for a reduced external field of 54 $V\,\mu m^{-1}$, which translates into a sensitivity of about $S_{1\%} = 0.14\,cm^2\,J^{-1}$. Thus, our fastest composite (5 wt % [84]PCBM, 56.6 $V\,\mu m^{-1}$ applied field, 0.3 $W\,cm^{-2}$ irradiance, $\tau_1 = 0.054$ s, $S_{1\%} = 4.8\,cm^2\,J^{-1}$) exhibits roughly a factor 44 faster response time and a factor 34 higher sensitivity.

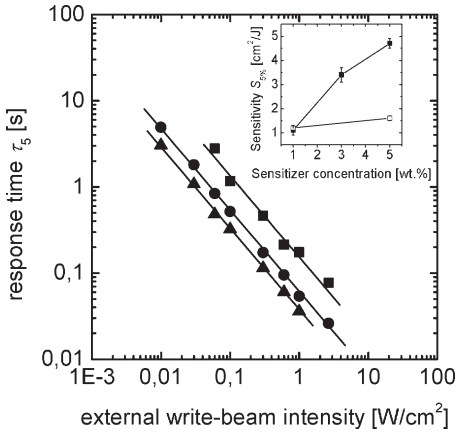

Figure 4. Response time τ_5 versus the external write-beam intensity, for composites containing 1 wt % (■), 3 wt % (●), and 5 wt % of [84]PCBM (▲) at $E_{ext} = 57\,V\,\mu m^{-1}$. The lines are fits to a power law. Inset: Sensitivity $S_{5\%}$ as a function of the sensitizer concentration of [84]PCBM (solid symbols) and TT-2324 (open symbols), calculated according to Equation 3 for $I_{ext} = 1\,W\,cm^{-2}$ and $E_{ext} = 56.6\,V\,\mu m^{-1}$.

From Figure 4 it is clear that increasing the sensitizer concentration and thus the absorption of the composite is to some extent equivalent to an increase of the intensity of the write beams. This finding is especially important for imaging applications that require fast holographic response times, but the maximum light intensity incident on the specimen is limited to prevent light-induced damage, which is particularly true for ophthalmic imaging.

For a direct comparison of both sensitizing agents, the sensitivity of the materials is plotted against the sensitizer content in the inset of Figure 4. For 1 wt % sensitizer, both materials exhibit a similar sensitivity, which is remarkable considering the fact that TT-2324 features a lower reduction potential (stronger acceptor compared to [84]PCBM), higher absorption and due to the lower molecular weight higher density of sensitizer molecules N_S in the composites of equal wt % content. The evident origin for the better performance is a higher charge generation quantum efficiency of the [84]PCBM sensitizer.

In conclusion, we have demonstrated for the first time PPCs with fast (i.e., millisecond) response time and complete internal diffraction efficiency at a recording wavelength of 1064 nm. The temporal performance of the fastest material described in this study corresponds to a factor 44 faster response than comparable materials at this wavelength. Thus, the material is highly promising for ophthalmic imaging applications. For the [84]PCBM sensitized PPCs, higher amounts of sensitizer led to increased steady-state values and faster response times, thus increasing the sensitivity of the materials. By contrast, due to the higher absorption of the TT-2324 sensitizer, the improvement in steady-state performance was compensated by the increase of the absorption loss, leading to unchanged sensitivity.

Experimental

Holographic Setup: The holographic properties of the materials were investigated in transmission geometry by a common degenerate four-wave-mixing (DFWM) and two-beam-coupling (2BC) setup, which is described in ref. [26]. The 1064 nm write beams (s-polarized, grating contrast $m = 1$) interfered in the material ($n = 1.7$), leading to a grating spacing of $\Lambda = 5.1\,\mu m$. The internal diffraction efficiency η_P (for p-polarized read-out) is calculated according to

$$\eta_p = \frac{I_D}{I_T + I_D} \quad (1)$$

with the transmitted intensity I_T and the diffracted intensity I_D of the read beam. The 2BC gain coefficient Γ_s is given by

$$\Gamma_S = [\ln(I_1/I_1(E=0))\cos\theta_1 - \ln(I_2/I_2(E=0))\cos\theta_2] \cdot d^{-1} \quad (2)$$

where $I(E = 0)$ indicates write-beam intensity without applied field. θ_1 and θ_2 denote the internal angles of write-beam 1 and 2 in the active material, respectively.

Field-dependent measurements were carried out by illuminating the material with both write beams at an external intensity of $1\,W\,cm^{-2}$ for 60 s at a given field before taking data points. For time-dependent measurements, the PPC was pre-poled for 300 s at $56.6\,V\,\mu m^{-1}$ without illumination before applying both write-beams to the material. For simple and straight forward comparison of the temporal behavior, τ_5-values were evaluated, stating the time necessary to reach an internal diffraction efficiency of 5%. In an analogous manner, τ_1-values (1% internal diffraction efficiency) were evaluated in one case to relate data in this work to a similar material at this spectral range. The sensitivity S was calculated according to

$$S = \frac{\sqrt{\eta_{ext}(t_{exp})}}{I_{WB,ext} \cdot t_{exp}} \quad (3)$$

whereas $\eta_{ext}(t_{exp})$ is the external diffraction efficiency after an exposure time t_{exp} with total external write beam intensity $I_{WB,ext}$.

The external diffraction efficiency η_{ext} is calculated from the internal diffraction efficiency η_{int} by taking absorption losses into account:

$$\eta_{ext} = \exp\left(-\frac{\alpha d}{\cos\alpha_1}\right)\eta_{int} \quad (4)$$

α denotes the absorption coefficient of the bulk PPC, d the active layer thickness, and α_1 the internal angle of the read-beam with regard to the sample normal.

Glass Transition Temperature: Differential scanning calorimetry measurements were carried out at a heating rate of $20\,K\,min^{-1}$, and measured between −50 and 180 °C.

Absorption Coefficient: α_{1064} was measured by trans-illuminating the samples perpendicular to the sample surface and applying Lambert–Beers law to the beam intensities, which were corrected for reflection losses.

Acknowledgements

This research was supported by the BMBF (DLR 50WB0730). The authors thank Rüdiger Sens (BASF) for providing TT-2324 and Ruth Bruker (University of Cologne) for taking the cyclic voltammograms.

Received: September 1, 2009
Revised: October 21, 2009
Published online: December 22, 2009

[1] E. Mecher, F. Gallego-Gomez, H. Tillmann, H. H. Hörhold, J. C. Hummelen, K. Meerholz, *Nature* **2002**, *418*, 959.
[2] M. Salvador, J. Prauzner, S. Köber, K. Meerholz, K. Jeong, D. D. Nolte, *Appl. Phys. Lett.* **2008**, 93.
[3] E. C. W. Lee, J. F. de Boer, M. Mujat, H. Lim, S. H. Yun, *Opt. Express* **2006**, *14*, 4403.
[4] K. Jeong, J. J. Turek, D. D. Nolte, *Appl. Opt.* **2007**, *46*, 4999.
[5] M. Cronin-Golomb, M. B. Klein, in: *Handbook of Optics*, Vol. II, 2nd ed. (Ed: M. Bass), McGraw-Hill, New York **1994**, Ch. 39.1
[6] K. Buse, F. Jermann, E. Krätzig, *Opt. Mater.* **1995**, *4*, 237.
[7] T. Bach, M. Jazbinsek, G. Montemezzani, P. Günter, A. A. Grabar, Y. M. Vysochanskii, *J. Opt. Soc. Am. B* **2007**, *24*, 1535.
[8] W. E. Moerner, S. M. Silence, F. Hache, G. C. Bjorklund, *J. Opt. Soc. Am. B* **1994**, *11*, 320.
[9] O. Ostroverkhova, W. E. Moerner, *Chem. Rev.* **2004**, *104*, 3267.
[10] M. Eralp, J. Thomas, S. Tay, G. Li, G. Meredith, A. Schülzgen, N. Peyghambarian, G. A. Walker, S. Barlow, S. R. Marder, *Appl. Phys. Lett.* **2004**, *85*, 1095.
[11] M. Salvador, J. Prauzner, S. Köber, K. Meerholz, J. J. Turek, K. Jeong, D. D. Nolte, *Opt. Express* **2009**, *17*, 11834.
[12] A. V. Vannikov, A. D. Grishina, *High Energy Chem.* **2007**, *41*, 162.
[13] J. G. Winiarz, L. M. Zhang, J. Park, P. N. Prasad, *J. Phys. Chem. B* **2002**, *106*, 967.
[14] K. R. Choudhury, Y. Sahoo, P. N. Prasad, *Adv. Mater.* **2005**, *17*, 2877.
[15] a) S. Tay, J. Thomas, M. Eralp, G. Q. Li, B. Kippelen, S. R. Marder, G. Meredith, A. Schülzgen, N. Peyghambarian, *Appl. Phys. Lett.* **2004**, *85*, 4561. b) S. Tay, J. Thomas, M. Eralp, G. Q. Li, R. A. Norwood, A. Schülzgen, M. Yamamoto, S. Barlow, G. A. Walker, S. R. Marder, N. Peyghambarian, *Appl. Phys. Lett.* **2005**, *87*, 171105.
[16] R. Bittner, K. Meerholz, in: *Photorefractive Materials and Their Applications II: Materials* (Eds: P. Günter, J.-P. Huignard), Springer Series in Optical Science, Vol. *114*, Springer, Berlin **2006**.
[17] B. Kippelen, in: *Photorefractive Materials and Their Applications II: Materials* (Eds: P. Günter, J.-P. Huignard), Springer Series in Optical Science, Vol. 114, Springer, Berlin/Heidelberg **2006**.
[18] J. Thomas, R. A. Norwood, N. Peyghambarian, *J. Mater. Chem.* **2009**, *19*, 7476.
[19] J. Schelter, A. Köhnen, J. Wies, K. Meerholz, G. F. Mielke, O. Nuyken, unpublished.
[20] F. B. Kooistra, V. D. Mihailetchi, L. M. Popescu, D. Kronholm, P. W. M. Blom, J. C. Hummelen, *Chem. Mater.* **2006**, *18*, 3068.
[21] H. Kogelnik, *Bell Syst. Tech. J.* **1969**, *48*, 2909.
[22] R. Bittner, K. Meerholz, G. Steckman, D. Psaltis, *Appl. Phys. Lett.* **2002**, *81*, 211.
[23] D. Van Steenwinckel, E. Hendrickx, A. Persoons, *J. Chem. Phys.* **2001**, *114*, 9557.
[24] S. Köber, F. Gallego-Gomez, M. Salvador, F. B. Kooistra, J. C. Hummelen, F. Mielke, O. Nuyken, K. Meerholz, *Photorefractive Effects, Photosensitivity, Fiber Gratings, Photonic Materials and More (PR) 2007*, OSA technical digest, TuC6.
[25] A. V. Vannikov, R. W. Rychwalski, A. D. Grishina, L. Y. Pereshivko, T. V. Krivenko, V. V. Savel'ev, V. I. Zolotarevskii, *Opt. Spectrosc.* **2005**, *99*, 643.
[26] E. Sliwinska, S. Mansurova, U. Hartwig, K. Buse, K. Meerholz, *Appl. Phys. B* **2009**, *95*, 519.